AUTOMATIC BOULDER IDENTIFICATIONS WITH DEEP LEARNING-BASED ALGORITHM: A CASE STUDY FOR TLANUWA REGIO OF BENNU. Y. Shimizu[1], R. Hemmi[2], H. Miyamoto[1], [1]School of Engineering, Department of Systems Innovation, Univ. of Tokyo, Tokyo, 113-8656, Japan (shimizu@seed.um.u-tokyo.ac.jp), [2]University Museum Univ. of Tokyo, Tokyo, Japan.

Introduction: Bennu is a near-earth asteroid having a spheroidal spinning-top shape [1]. NASA's Origins, Spectral Interpretation, Resource Identification and Security-Regolith Explorer (OSIRIS-REx) mission [2] revealed that this B-type asteroid [3] is covered by hydrated and dark (low albedo) surface materials [e.g., 4]. The observed high-porosity is interpreted to indicate its rubble-pile structure [5].

Despite its small-size (<500 m in diameter), high-resolution images (better than several cm per pixel) from OSIRIS-REx Camera Suite (OCAMS) [6] resolved an unexpected surface diversity of Bennu [4] with a variety of topographic/geologic features, including an equatorial bulge, longitudinal ridges and troughs, craters or crater candidates with circular depressions, and lineaments [5, 7].

The existence of abundant regolith and fragmented rock particles (boulders, cobbles, and pebbles) may suggest the influence of impact or thermal processes occurring on the surface after its formation [8]. Images obtained with OCAMS show the signs of other geological processes. Those include particle ejections from the surface due to its low escape velocity [9], and mass wasting, where the surface materials move to topographic lows. These would lead to the accumulations of clusters of boulders, depletion of small craters, and/or infilling of large craters [10]. Analyzing the sizes and spatial distributions of rock particles and regolith of Bennu can thus contribute to understanding the origins and evolutions of this diverse and active surface.

Identification of Rock Particles: Previously, particles identification was manually conducted by fitting polylines to their longest axis dimension [11], or ellipses to their shapes [12]. Boulder outlines are generally blurred and difficult to distinguish from the background due to irregular particle shapes, overlapping particles, and image resolution limits, making the analysis time-consuming and challenging, which will result in a lack of reproducibility. Therefore, a method to analyze numerous rock particles with objectivity and reproducibility should be established. Here, we develop a deep learning-based computational approach for the automatic identifications of rock particles. Then we apply this method to boulders in Tlanuwa Regio, a large boulder-rich area on Bennu's surface, and discuss its origins and evolutions.

Tlanuwa Regio: The global rock abundance on Bennu's surface is not uniform [7]; there are concentrations of boulders in certain places, and Bennu's surface can be classified into at least two geologic units, smooth and rugged units [13]. Tlanuwa Regio is a rugged region located in 9.0–66.2° S and 223.13–300.26° E having an area of ~0.928 km^2. It includes the area where rocks are the most abundant on Bennu [7], and thus we choose the Tlanuwa Regio to be studied with our algorithm.

Automatic Identification Algorithm: To obtain information on the size, shape, position, and orientation of each particle, we design a method to perform instance segmentation tasks, which can distinguish individual particles from the background in pixel level (pixel-wise). Mask R-CNN with ResNet-101 [14] is used for the model, and hyperparameters are optimized to identify numerous rock particles in grayscale images, which is entirely different from general object detection.

Training of The Model: For the effective identification of rock particles, lighting conditions of images are the most critical; solar phase angles should be appropriate (~30-50°) and emission angles (angles between a spacecraft and a normal vector of the surface) should be small (<40°) to determine outlines of particles from the direction perpendicular to the surface (nadir). To fulfill this requirement, OCAMS images obtained during the Baseball Diamond (BBD) imaging campaign in the Detailed Survey mission phase [2] are selected to train the model. 26 images are prepared for a training dataset, while 8 images are prepared for a validation dataset. Additionally, 24 images of Tlanuwa Regio are used as a test dataset for evaluating the accuracy of the model.

By carefully identifying each rock profile with a manual analysis, we finally obtain >40,000 outlines of rocks. With this dataset, the model is trained.

Evaluation of the Model: Fig. 1 shows an example of automatic identification. To evaluate the trained model, we use three metrics: precision, recall, and F-value. They are defined as $precision = T_p/(T_p + F_n)$, $recall = T_p/(T_p + F_p)$, and $F\text{-}value = 2precision \cdot recall/(precision + recall)$, where T_P is the true positive, which shows the number of objects estimated as a particle by both the automatic/manual analyzes, and F_P is the false positive, which shows the number of objects automatically estimated as a particle, but not

manually. F_n is the inverse of F_P. The model achieves a recall of 81.0 %, precision of 80.3 %, and F-value of 80.6 %. Note that particles with <12 pixels in diameter are excluded from the results in both automatic/manual analysis, because small particles are often blurred mainly due to image resolution limits, which makes difficult to determine the outline even for manual analysis.

Boulder Analysis in Tlanuwa Regio: For identifying rock particles in Tlanuwa Regio, 80 OCAMS images (~5 cm/pix) obtained during the BBD mission phase are prepared. By using our algorithm, >100,000 particles are identified automatically. Each image has overlapping areas with other images, so we review overlapping identifications on a 217,032-facet shape model (v20 PTM) derived from OSIRIS-REx Laser Altimeter (OLA) [15]. Finally, ~20,000 particles are recorded, and they are mapped on the shape model by using Small Body Mapping Tool (SBMT) [16] (Fig. 2).

Size/Shape Distributions and Orientation: We calculate the cumulative size-frequency distribution of rock particles in Tlanuwa Regio. It is fitted with power-law distribution having a power-law index of -2.2.

By measuring the largest (a) and second the largest (b) dimensions, the ratio of b/a is derived for each particle, showing the mean ratio of 0.63. This result is consistent with the value of Eros, Itokawa and Ryugu [17], which suggest the origins of particles can be attributed to impact processes compared to the shape distribution obtained in laboratory impact experiments [18].

The orientation of each particle is also obtained (Fig. 2). Here 0° shows the longest axis is parallel to the direction of the equator, and the orientation is defined counterclockwise from this origin. The global orientation trend in Tlanuwa Regio shows that most particles have orientations parallel to the equator. With the hypothesis that the longest axis is preferentially oriented transverse to the gravel migration [19], and Bennu's geopotential trend, where the current potential is the highest at the poles and the lowest at the equator [20], this trend can indicate that surface materials have dominantly moved from the midlatitude to the equator in Tlanuwa Regio.

References: [1] Nolan M. C. et al. (2013) *Icarus* 226, 629-640. [2] Lauretta D. S. et al. (2017) *Space Sci. Rev.* 212, 925-984. [3] Hergenrother C. W. et al. (2013) *Icarus* 226, 663-670. [4] Lauretta D. S. et al. (2019) *Nature* 568, 55-60. [5] Barnouin O. S. et al. (2019) *Nat. Geosci.* 12, 247-252. [6] Rizk B. et al. (2018) *Space Sci. Rev.* 214, 26. [7] Walsh K. J. et al. (2019) *Nat. Geosci.* 12, 399. [8] DellaGiustina D. N. et al. (2019) *Nat. Astron* 3, 341-351. [9] Lauretta D. S. et al. (2019) *Science*, 366, eaay3544. [10] Jawin E. R. et al. (2020) *JGR* 125, e2020JE006475. [11] Burke K. N. et al. *Remote Sens.* 13, 1315. [12] Michikami T. et al. (2019) *Icarus* 331, 179-191. [13] Jawin E. R. et al. (2020) *LPSC 52nd Abs.* #2022. [14] He K. et al. (2017) *Proc. IEEE Int. Conf. Comput.* 2961-2969. [15] Barnouin O. S. et al. (2020) *PSS* 180, 104764. [16] Ernst C. M. et al. (2018) *LPSC 49th Abs.* #1043. [17] Michikami T. & Hagermann A. (2021) *Icarus* 357, 114282. [18] Michikami T. et al. (2010) *Icarus* 207, 277-284. [19] Miyamoto H. et al. (2007) *Science* 316, 1011-1014. [20] Scheeres D. J. et al. (2019) *Nat. Astron.* 3, 352-361.

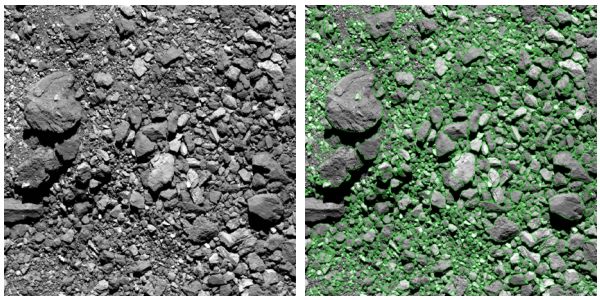

Fig. 1. OCAMS image (left: ocams20190405t182630s769_pol_iofl2pan_83523) and automatically identified particles (right).

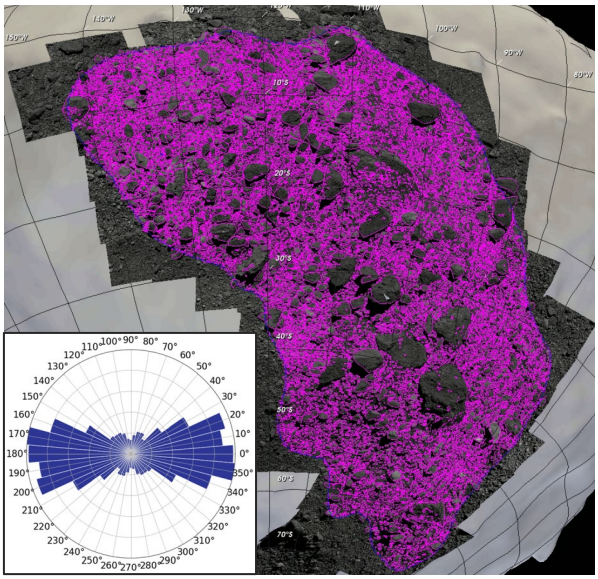

Fig. 2. Mapped rock particles and the global orientation trend (lower left). 0° shows the longest axis is oriented in East-West direction, and data is symmetrical to 0°– 180°.